Novel Proteasome Activators for the Study of Proteasome Population Dynamics and MHC-I Peptide Generation

Novel Proteasome Activators for the Study of Proteasome Population Dynamics and MHC-I Peptide Generation

Jonathan Nolasco-Sanchez

A Thesis in the Field of Biology

for the Degree of Master of Liberal Arts in Extension Studies

Harvard University

May 2020

Abstract

The 26S proteasome is the major protease found in eukaryotic cells. It is responsible for the degradation of most proteins into a mixture of heterogeneous small peptides. Proteasomes are tightly regulated, relying on ubiquitin tagging for substrate loading and ATP hydrolysis for protein degradation. A number of proteasome activators have been previously described. Here, I show that the UBL domain of Rad23a is a potent activator of the double-capped and single-capped 26S proteasome but an inhibitor of the 20S. Additionally, peptide presentation by MHC-I increases with heat shock, which also activates proteasomes.

“The world must know, from this time forward that the Mexican-American is coming into his own right. You are winning a special kind of citizenship; No one is doing it for you—you are winning it yourselves—and therefore no one can ever take it away.”

Robert F. Kennedy.
Harvard College, Class of 1948

Author's Biographical Sketch

Jonathan is a California native who earned his Bachelors of Science in Microbial Biology from the University of California, Berkeley. For the last four years, in addition to completing his Master's work, he has worked at several Cambridge-based biotechnology companies. His work has encompassed scale-up production of monoclonal antibody therapeutics, development of CRISPR-Cas9 based therapies, as well as nucleotide vaccine research for influenza and pandemic viruses. A former distance runner and collegiate rower, Jonathan enjoys spending time outdoors and baking.

Dedication

Para mis padres, sin los cuales ningunos de mis éxitos serían possible.

Acknowledgments

I'd like to thank all the members of the Goldberg lab for guiding my thinking and growth as a scientist. Special thanks to Dr. Galen Collins and Dr. Alfred Goldberg who served as my mentors and oversaw my research and writing. Galen, thank you for all the help; this thesis would not have been possible without your mentorship. I'd also like to thank Dr. Jeff Colbert from the Kenneth Rock lab for providing flow cytometry training and the HeLa cells used in this work.

Warm thanks to Michael, Shoman, and Pema for providing love and support throughout the years.

Table of Contents

List of Figures

Chapter I.

Introduction

Protein degradation and protein synthesis are tightly regulated in all cells. In eukaryotic cells, the proteasome is central to the degradation of most intracellular proteins. 20S proteasomes are large barrel-shaped protease complexes present in eukaryotes, archaea, and some bacteria (Schrader et al., 2009). In eukaryotes, hexameric ATPase rings regulate substrate access to the 20S proteases (Fort et al., 2015). The eukaryotic ATP-dependent proteasome is referred to as the 26S proteasome, consisting of a 20S core particle plus one or two 19S regulatory particles (RP) (Lowe et al., 1995).

Proteasomes are not the only protein degradation pathway present in eukaryotic cells. Eukaryotes also degrade cellular proteins via the lysosomal system. However, unlike proteasomes which are selective in their degradation, lysosomes— which are membrane bound organelles—are often non-specific in which cytosolic proteins they degrade via autophagy (Cooper, 2019). 26S proteasomes degrade proteins into a mixture of heterogeneous peptides (2- 20 amino acids long), but do not degrade proteins directly to free amino acids (Goldberg et al., 2002). The ubiquitin-proteasome system (UPS) relies on ubiquitin tagging for the selection of proteins to be degraded by the 26S proteasome. UPS-mediated degradation is responsible for about 80% of intracellular protein breakdown (Collins and Goldberg, 2017). The reliance on ubiquitin tagging allows the UPS to selectively destroy regulatory and signaling proteins, as well as proteins that are misfolded, damaged, or incompletely translated. Consequently, proteasomes play a key role in maintaining protein turnover in cells and maintaining

proper cell health (Schmidt and Finley, 2014). In addition to simply degrading proteins, the 26S proteasome generates peptides which bind to the MHC-I for antigen presentation to the immune system (Liepe et al., 2016; Scruggs et al., 2012).

Three proteasome-targeting drugs have been approved by the FDA (Food and Drug Administration), all of which inhibit the 20S proteases. For many diseases (e.g. Alzheimer's disease, Parkinson's Disease, amyotrophic lateral sclerosis), the accumulation of damaged or misfolded proteins is closely linked to disease progression. Therefore, mechanisms by which to stimulate proteasome activity is an active area of research. Proteasomes can be activated by genetic, chemical and post-translational approaches (Chondrogianni, et al., 2014). To better understand the mechanism of proteasome activation and the biological consequences of stimulating the UPS, my work will use two recently discovered methods of activating the proteasome - a UBL (ubiquitin-like) domain and increased temperature (heat shock).

The first part of my thesis investigates whether the UBL domain activates the 26S proteasomes with either one or two 19S regulatory particles similarly. The second part of my thesis aims to elucidate the relationship between heat shock-mediated increase in protein degradation and peptide presentation on major histocompatibility complex class-I (MHC-I) on the cell surface.

Proteasome Structure and Activity

The 20S proteasome is composed of two α-rings and two β-rings. The α-rings and β-rings are each composed of seven α and β subunits, respectively, and form a barrel-like structure consisting of two β-rings sandwiched between two α-rings ($\alpha_{1-7}\,\beta_{1-7}\,\beta_{1-7}\,\alpha_{1-7}$.) The catalytic sites of the 20S proteasome are present in duplicate, and are located in the β_1, β_2, and β_5 subunits. Specifically, the β_5 subunits cleave the peptide bonds following hydrophobic residues (chymotrypsin-like), the β_2 subunits cleave after basic amino acids (trypsin-like), and the β_1 subunits cleave after acidic amino acids (caspase-like) (Kisselev et al., 2006). Such diverse catalytic activity allows proteasomes to degrade most intracellular proteins almost completely.

19S regulatory particles (19S RP) can bind to the α-rings on either one or both ends of the 20S core particle. The 19S RP itself is made up of two sub-complexes, often referred to as the base and the lid. The base is made up of six ATPase subunits (Rpt1-Rpt6) that form a ring and associate with four non-ATPase subunits (Rpn1, Rpn2, Rpn10 and Rpn13). Rpn1, Rpn10 and Rpn13 bind ubiquitin tagged proteins. Rpn10 contains a short helical sequence called the ubiquitin-interacting motif (UIM), Rpn13 has a pleckstrin-like receptor for ubiquitin (Pru) domain, and Rpn1 has the toroid 1 and toroid 2 (T1, T2) sites (Schreiner et al., 2008; Chen et al., 2016). The lid is made up of nine Rpn subunits (Rpn3, Rpn5-9, Rpn11-12, and Rpn15). Rpn11 deubiquitinates substrates entering the proteasome while the functions of the other lid sub-complexes remain unclear. The removal of ubiquitin from proteasome bound proteins, prior to their

degradation, is carried out by several deubiquitinating enzymes (DUBs), most notably Rpn11, Uch37, and Usp14 (Collins and Goldberg, 2017).

Additionally, Kim and Goldberg found that the ubiquitin-like (UBL) domain of Usp14 can activate proteasomes. UBL domains had been previously described for their abilities to bind to proteasomes (at Rpn1, Rpn10, and Rpn13), and in their study Collins and Goldberg found that several UBL domains, besides Usp14, enhance proteolytic activity of proteasomes (Collins and Goldberg, 2020). Experimental data indicates that UBL domains on many proteins can activate the 26S proteasome in the same manner that ubiquitin chains activate the 26S proteasome (Collins and Goldberg, 2020). Upon recognition of the ubiquitin tagged proteins, or UBL domain by the proteasome the 19S unfolds, deubiquitinates, and translocates the substrate into the interior of the 20S where degradation occurs (Collins and Goldberg, 2017).

Proteasome Activation

The proteasome is highly selective for its targets and tightly regulated. Structural elements of the 26S proteasome, such as the narrow gated pore formed by the α-subunits, prevent proteins from entering. Additionally, the labeling of substrates by ubiquitin is a tightly regulated process, without which proteasomal degradation is limited. The ubiquitination of a substrate occurs in a series of sequential steps involving three enzymes. First, the ubiquitin activating enzyme (E1) causes ATP to make the ubiquitin molecules more reactive by forming a thioester between a cysteine at its active site and the C-terminus of ubiquitin. The E1 then transfers the activated ubiquitin to a cysteine of ubiquitin conjugating enzyme (E2). The E3 binds to the substrate and also the loaded E2

to form an E2-E3-substrate complex. This complex catalyzes the formation of an isopeptide bond between α-carboxyl group of the ubiquitin and the ε-amino group of a lysine in the substrate (Weissman, 2001).

The N-termini of the proteasome's α-subunits prevent proteins from accessing the catalytic core. Therefore proteasomes are considered latent, as access to the catalytic sites is only granted when an activator of the 26S proteasome triggers gate opening. Natural activators of proteasomes include the 19S RP, PA200, and PA28. A common feature of these activators is their binding to the α-ring of the 20S subunit thereby regulating gate opening. Proteasome activators therefore increase proteolytic activity by increasing the number of active proteasomes. Proteasome activity is also determined by the catalytic subunits, as well as the chaperones involved in proteasome assembly which determine how many proteasomes exist in cells. PA28 and PA200 are activators of latent 20S proteasomes. Both PA28 and PA200 complex with the 20S and trigger a conformational change in α-subunits thereby activating the proteasome. However, their functions are distinct: PA28 is an ATP-independent activator that stimulates peptide degradation but not intact or polyubiquitinated proteins, whereas PA200 is a regulator of proteasome proteolytic activity (though its specific role in vivo is partially understood) (Blickwedehl et al., 2008; Shibatani et al., 2006).

There are several distinct activators of the proteasome which are capable of activating proteasomes in vitro. A useful activator of purified 20S proteasomes is sodium dodecyl sulfate (SDS), which was shown to activate the 20S at low concentrations but inhibits at higher concentrations. Similarly, the slow hydrolysable ATP analog, ATPγS, increases proteasome activity by trapping the 26S proteasomes in a constituently active

ATP-bound form with the gate into the 20S open (Sledz et al., 2013; Collins and Golberg, 2017).

Proteasome Regulatory Caps and their Roles

Access to the catalytic β subunits is restricted by a gate composed of the N-termini of the α-subunits that move in and out of a narrow pore that forms the opening of the 20S (Tanaka, 2009). When the 26S proteasome is activated (by 19S RP caps, or by alternative activators such as PA200 or PA28) the N-termini of the α-rings extends outward, thereby opening the gate and granting the unfolded proteins access to the catalytic β-subunits, which subsequently leads to protein degradation (Collins and Goldberg, 2017).

Structural and biochemical analysis reveal that three of the six ATP dependent proteasome regulators contain a conserved C-terminal HbYX motif (where Hb stands for a hydrophobic residue; Y for tyrosine; and X for any amino acid) which is essential for ATP-dependent gate opening (Rabl et al., 2008). ATP independent activators disrupt the hydrogen bond interactions of the tightly closed α-rings within the 20S core, widening the entrance by which substrates enter the core, and ultimately stabilizing the 20S in the substrate processing state. In spite of this robust and frequently referenced biochemical activation of proteasomes by ATP independent pathways, the biological roles of these activators are poorly understood (Stadtmuller and Hill, 2011).

Interestingly, regulatory particles are not the only way proteasomes acquire specificity; the 20S core can also change its subunit makeup in response to inflammatory signaling molecules. The different isoforms of the 20S are 1) constitutive proteasomes,

described above, which make up the bulk of 20S core particles, 2) immunoproteasomes, found in immune cells or formed in all cell types in response to IFN-γ or TNF-α signaling, in these 20S particles the β_1, β_2, and β_5 subunits are replaced by β1i, β2i, and β5i which generate different peptides for MHC-I presentation, 3) intermediate proteasomes, which contain a mix of subunits from the constitutive proteasome and the immunoproteasome which enhances peptide generation for MHC-I, 4) thymoproteasomes, found only in cortical thymic epithelial cells and contain the unique β5t subunit (produce distinct peptides for cluster of differentiation 8 (CD8) selection), and finally 5) spermatoproteasomes, present in the testes and contain the unique α4s subunit which plays a role in spermatogenesis (Morozov and Karpov, 2018). I will focus on constitutive proteasomes which contain a 20S core and one or two 19S RP.

Proteasomes exist in cells in various compositions: A single-capped (the 26S), a double-capped (occasionally referred to as the 30S), and uncapped proteasome (20S). Structural research completed by Fonseca and Morris suggests that both the single-capped and double-capped proteasome behave the same upon activation: binding of ubiquitin to Usp14 or Uch37 of the 19S RP triggers the gate-opening (Fonseca and Morris, 2008; Peth et al., 2009).

Further work by Asano and colleagues determined that roughly 20% of proteasomes are active in the absence of proteotoxic stress (Asano et al., 2015). They analyzed intact hippocampal neurons using electron cryotomography. Moreover, they determined the overall distribution of single-capped proteasomes (1156 particles, 73%) and double-capped proteasomes (425 particles, 27%). Electron cryotomography visualized their samples with a resolution of 47 Å, this high resolution imaging in

combination with in silico slicing lead them to conclude that both RPs act independent of each other in a double-capped proteasome (Asano et al., 2015). This observation suggests that both the single-capped and double-capped 26S proteasomes are activated in the same manner: the binding of ubiquitin (or other activators) to the 19S RP triggers subsequent rearrangement of 20S subunits. Binding of ubiquitinated proteins to the 19S RP leads to the opening of the 20S gate thereby granting access to the proteolytic core of the 20S. The catalytic core (β1, β2, β5, β6, and β7) is made accessible by the displacement of the α1, α4, α5, α6, α7, of the 20S. This is particularly intriguing, as both the single-capped and double-capped proteasome are both present in cells but the exact function of each distinct conformation, as well as their relationship with one another, has not been well established. In a separate study of double-capped proteasomes Berko and colleagues concluded that Rpn13 is only present on one side of a double-capped proteasome. They hypothesized that this asymmetry found in double-capped proteasomes leads to directional processing of peptides (Berko et al., 2014).

While the majority of proteasomes are inactive in cells and require an activating signal, activation of latent proteasomes can occur by the binding of ubiquitinated proteins to Usp14 or Uch37, as well as the binding of UBL domains to Rpn1. The works of Asano and colleagues and Berko and colleagues suggest that having a double-capped proteasome may result in more active proteasomes due to an increase of binding sites for activating molecules. By studying the effects of proteasome activation by UBL, I hope to compare rates of activation between different proteasome populations; specifically, 20S, 26S double-capped, and 26S single-capped.

MHC-I and the Proteasome (Structure, Function, and Proteasome Antigen Generation)

Most nucleated mammalian cells express MHC-I molecules on their cell surface. MHC-I molecules present peptide fragments which are used by T cells to monitor cell health. Foreign or aberrantly produced proteins, when degraded by the 26S proteasome, result in new, abnormal peptides on the surface. When these neo-antigens are presented by MHC-I surface molecules they are recognized by T cells. Specifically, CD8+ T cells bind to the antigen presenting cell and trigger apoptosis by releasing the cytotoxic protein granzyme, or the pore-forming perforin protein (Bennette et al., 2014).

MHC-I molecules are transmembrane heterodimer proteins composed of a heavy chain and a light chain. The heavy chain is composed of α-chains with three domains (α1, α2, and α3). The α1 and α2 domains form a globular protein on which the peptide-binding groove is located. The peptide-binding groove is composed of β-pleated sheets which serve as the floor for the peptide to bind. In turn, the peptide-binding groove is bounded by two helical regions (Bennette et al., 2014; Hewitt, 2003). The third alpha domain (α3) anchors the MHC-I molecule to the cell membrane. The light chain, beta-2 microglobulin (β2m), noncovalently associates with the heavy chain. β2m is a 12-kDa protein that, when associated with the heavy chain, provides structural stability to the peptide-binding groove. β2m also plays a pivotal role in eliciting a CD8+ T-cell response. β2m interacts with the co-receptors of CD8+ T-cells and facilitates the interaction of the MHC-I molecule and CD8-T (Bennette et al., 2014; Hewitt, 2003). Unsurprisingly, β2m deficient mice show a significant decrease in CD8+ T-cells (Li et al., 2016). Importantly, the MHC-I peptide-binding groove has conserved tyrosine residues that form the helical

closure of the floor (i.e. peptide binding site). These tyrosine residues only allow peptides that are between 8 and 9 residues long to bind to MHC-I molecules (Kisselev et al., 1999).

The proteasome is the source of most antigen peptides as seen when the proteasome is inhibited (Rock et al., 1994). Even proteasome generated peptides that are too small (< 9 residues) or too large (> 10 residues) to bind to MHC-I are further trimmed by other peptidases to the proper length. The 26S proteasome generates peptides of 2-20 amino acid length, paired with the preferential cleavage of proteins by the immunoproteasomes which generate increased amounts of C-terminal anchor residues strongly support the role of the proteasome in the MHC-I peptide presentation pathway (Rock et al., 2016). Furthermore, the immunoproteasome generated C-terminal anchor residues bind to specific pockets of the MHC-I groove facilitating the binding of the peptide to the MHC-I epitope. Foreign proteins produced by intracellular bacteria or viruses are degraded to peptides by the proteasome in the cytosol. The resulting peptides are translocated from the cytosol to the ER by the ATP dependent transporter associated with antigen processing (TAP) protein complex. Once inside of the ER lumen, tapasin, the peptide loading chaperone, along with TAPBPR load the peptide to the empty MHC class I molecule. Once a peptide is bound to MHC-I, the MHC-I-peptide complex is transported to the Golgi and further packaged into a secretory vesicle for cell surface presentation (Rock et al., 2016).

Furthermore, evidence presented by Rock and colleagues in their seminal 1994 paper strongly supports the role of the 26S proteasome in the MHC-I pathway (Rock et al., 1994). When Rock and colleagues expressed ovalbumin in murine B-lymphoblastoid

cells, they found that the proteasome was needed for these cells to present the ovalbumin derived peptide, SIINFEKL, on the cell surface. Cells expressing ovalbumin and treated with the proteasome inhibitor MG-115 (a potent inhibitor of 20S chymotryptic activity) had reduced SIINFEKL presentation. However, if cells expressed just the processed peptide SIINFEKL, instead of the precursor protein ovalbumin, this antigen was still presented on the surface even when proteasomes were inhibited with MG115. Because proteasome inhibition led to a decrease in MHC-I presentation without affecting the rest of the MHC-I pathway (i.e. TAP, tapasin, TAPBPR etc. functioned normally), this finding highlights the role of the proteasome in the generation of peptides for MHC-I presentation (Rock et al., 1994). The effects of proteasome inhibition are well studied. Inhibiting the proteasome induces 1) cell cycle arrest, 2) apoptosis, 3) ER stress, 4) inhibition of NF-kB, and 5) inhibition of DNA repair (Fabre et al., 2012). Specifically, proteasome inhibition leads to a buildup of polyubiquitinated proteins which eventually form aggregates, called aggresomes, which are slowly cleaved by autophagy (Hideshima et al., 2005). Inhibiting the proteasome also results in cell cycle arrest at G2/M via the inhibition of cyclin dependent kinases, cyclin D, cyclin E, and Cdc25 (Kisselev and Goldberg, 2001).

Conversely, the downstream effects of proteasome activation via exogenous stimuli have not been widely studied. Based on the pioneering work completed by Rock and Goldberg, my thesis work will look at the effects of proteasome upregulation on MHC-I presentation. Lee and colleagues described the role of the zinc finger proteins ZFAND5, and ZFAND2a in the stimulation of 26s proteasomes via the enhancement of gate opening of the 20S. Both zinc fingers are expressed during disruptions of protein

homeostasis. They specifically found that ZFAND5 is capable of stimulating protein degradation by the UPS pathway (Lee et al., 2018). Recently, Lee and Goldberg found that heat shock stimulates 26S proteasomes as a response to accumulation of ubiquitinated proteins (Lee and Goldberg, 2020). Earlier work had described the rise of cellular protein degradation following a "heat shock" of cells, however, the proteasome was not established as the cause (Parag et al., 1987). The established crosstalk between the proteasome, and MHC-I suggests that activating proteasomes by using heat shock will lead to an upregulation of MHC- I antigen presentation. Conceivably, this surge is mediated by the boost in proteasome generated peptides, thereby giving MHC-I a larger pool of peptides to which it can bind. The implications of such findings could be impactful in the field of immunotherapy, specifically for CAR-T therapy and immune checkpoint inhibitors. If, in fact, stimulating the proteasome leads to more MHC-I antigen presentation, then concordantly, stimulating the proteasome in cancerous cells would lead to a larger pool of antigens and a larger pool of potential targets for the CAR-T cells.

To that end, this work ties the findings of Asano and colleagues (in the absence of a proteotoxic environment only 20% of proteasomes are active), and Rock and Goldberg (the proteasome is the primary generator of MHC-I peptides) to study the effects of MHC-I peptide presentation when proteasomes are stimulated by a proteotoxic stress (heat shock) which causes unfolding of many cell proteins.

Chapter II.

Materials and Methods

Labeling Proteasomes with the Activity Probe MVB-127

To assess the effects of the UBL domain of Rad23a (provided by Goldberg lab, Boston MA) on the activation of single-capped and double-capped 26S proteasomes, 12 nM purified 26S proteasomes from Mouse Embryonic Fibroblasts (MEF) (provided by Goldberg lab, Boston MA) were incubated at 37°C for 0 - 4.5 hours in a reaction buffer (25 mM HEPES (pH 7.5), 100 mM KCl, 5 mM MgCl2, 0.1 mM ATPγS, 1 mM DTT) and 25 nM of the activity probe MV-127. 500 nM Rad23a-UBL, or an equivalen volume of ultrapure water, were included in the reactions as indicated. This experiment was conducted as a reverse time course with all materials kept on ice until the start of their incubation. At the end of each time point, MG-132 (provided by Goldberg lab, Boston MA) was added at a final concentration of 1.66 μM to all reactions to stop further proteasome activity.

Resolution of Proteasome Sub-Populations by Native Gel Electrophoresis

To observe the activity of the different 26S proteasome sub-populations, the reactions from step 1.1 were analyzed by native PAGE (polyacrylamide gel

electrophoresis). Native PAGE separates proteasomes without denaturing or reducing buffers, which maintains the tertiary structures (folding of subunits) and quaternary structures (assembly of the multi-subunit complexes) of the samples. Thus, with Native PAGE single-capped, double-capped and 20S proteasomes can be distinghuished. Reactions generated in step 1.1 were diluted 4 to 1 in 4× Native PAGE Sample Buffer (Novex BN2003). Samples were loaded on a 3-8% Tris-Acetate PAGE (ThermoFisher Scientific EA0375BOX) and were run at a constant current of 10 mA overnight at 4°C with chilled running buffer (1x Native PAGE running buffer (Novex BN2003) supplemented with 5 mM MgCl2, 1 mM ATP, 0.5 mM DTT).

Imaging Native PAGE

Proteasome populations were labeled by MVB-127 and the fluorescent signal was captured using a GE Amersham AI600 RGB imager using 520 nm excitation and a Cy3 filter using auto-gain. Background noise was subtracted using the "rolling ball" method with the IQTL software package (GE LifeSciences).

Western Blot of Native PAGE

Proteins, separated by Native PAGE, were transferred onto a 0.45 μm PVDF membrane (Millipore Sigma IPFL00010) at 4°C overnight in 1× Tris-Glycine buffer (without methanol) with a constant current of 30 V. The PVDF membrane was blocked with Odyssey blocking buffer (Li-COR 927-40000) for one hour. The membrane was then incubated overnight with the primary antibody prep (0.1%(w/v) Tween-20, 1:1,000

Sug1 antibody (ThermoFisher Scientific MA3-087), 1:1,000 PSMB5 antibody (Bethyl A303-847A), in Odyssey blocking solution at 4°C. The PVDF membrane was washed with TBS-T (20 mM tris, 150 mM NaCl, 0.1 % (w/v) Tween 20) for 20 minutes (4 x 5 minute washes on a rocker). The PVDF membrane was then incubated on a rocker with the secondary antibody mix (0.1 % (w/v) Tween 20, 0.01 % (w/v) SDS, 1:15,000 Goat anti-rabbit 800, 1:20,000 anti-mouse (LT) 680, Odyssey blocking solution) for 45 minutes protected from light. The PVDF membrane was then washed for 20 minutes with TBST (4x5min washes on rocker) and finally rinsed in TBS (20 mM Tris, 150 mM NaCl). The membrane was imaged with an excitation of 680 nm and 800 nm (Li-COR Odyssey CLx) with automatic gain on the fluorescent detection and no focus off-set.

Peptidase Assay of Purified Proteasomes

2 nM of purified 26S proteasomes from Mouse Embryonic Fibroblasts (MEF) (provided by Goldberg lab, Boston MA) was incubated with indicated concentrations of ATP (or ATPγS) and Rad23a UBL in 50 mM Tris-HCl pH 7.6, 100 mM KCl, 0.5 mM MgCl2, 25 ng/μL bovine serum albumin, 10 μM ac-Nle-Pro-Nle-Asp-AMC (nLPnLD). 100 μL of the reaction was plated in triplicate in a black 96-well plate. The generation of cleaved 7-amino-3-methylcoumarin (AMC) fluorescent signal is measured using a plate reader (λex = 380 nm, λem = 460 nm once per minutes for 42 minutes at 37°C). AMC is a fluorescent molecule that is conjugated with the nLPnLD peptide., Attached to the nLPnLD peptide is the AMC fluorescent moiety, which is quenched when attached to peptide but can be excited when cleaved, allowing for fluorescence emission.

Statistical Analysis

Statistical analysis completed using Graph Pad Prism version 8. Significance was tested with an unpaired, homoscedastic Student's T-test using a p-value of 0.05 as the cut-off value.

MHC-I Presentation

Cell Culture

HeLa cells (Provided by Goldberg lab, Boston MA), HeLa H2-K^b cells (Provided by Rock lab, Worcester MA), and HeLa H2-K^b cells expressing non-secreted ovalbumin (NS-OVA) (Provided by Rock lab, Worcester MA), were cultured in RPMI 1640 media with L-glutamine (Corning Life Sciences 10-040-CV) supplemented with 10% fetal bovine serum (Sigma 12103C-100ml). All cells were cultured at 37°C with 5% CO_2 in 6 cm plates until 80% confluent. Selection for H2-K^b was maintained with 20 μg/mL of hygromycin (ThermoFisher Scientific 10687010) for a week and discontinued the morning prior to the start of experiments.

Heat Shock Induction and Cell Lysate Preparation

Cells were washed and pre-warmed media (43°C) was added. The cells were then moved to a 43°C incubator. Experiments were completed as a reverse time course with the indicated time points. Cells were collected on ice by scraping into 1.5 mL tubes after washing with 5 mL chilled 1× PBS. Cells were pelleted at 100 ×g for 2 minutes at 4°C. The pelleted cells were resuspended in 150 µL of 25 mM HEPES (pH 7.5), 5 mM MgCl2, 10% (w/v) glycerol, 1 mM ATP, 1 mM DTT, 1 mM Phenylmethylsulfonyl fluoride (PMSF) (Sigma, 10837091001) , 10 µM N-Ethylmaleimide (NEM) (Sigma, E3876-5G) and sonicated on ice with 4 × 6 second bursts at 12 µm amplitude. Lysates were clarified by centrifugation at 10,000 ×g at 4°C for 10 minutes. The supernatant was collected, then frozen at -80°C for later use.

Bradford Assay for Protein Concentration

Protein standards where made with bovine serum albumin (BSA) (ThermoFisheser Scientific 23209) diluted in water with a working range of 0 - 2000 µg/mL. The Coomassie reagent (ThermoFisher Scientific 23236) was equilibrated at room temperature for 1 hour. Once equilibrated, 750 µL of Coomassie reagent was mixed with 25 µL of sample or standard. The samples were incubated for 10 minutes at room temperature and loaded to a clear 96 well bottom plate in triplicate. The absorbance was measured at 595 nm with a plate reader (Molecular Devices).

Peptidase Assay in Cell Lysates

All samples were diluted to equal protein concentrations. 1% (w/v)- 4% (w/v) of sample was added to 50 mM Tris-HCl pH 7.5, 100 mM KCl, 1 mM ATP, 5 mM MgCl2, 25 ng/μL BSA, and 10 μM suc-LLVY-AMC Samples were loaded in triplicate to a black 96 well flat bottom well plate (Greiner Bio-one). The generation of cleaved AMC fluorescent signal was measured at 37°C using a plate reader (Molecular Devices) for 42 minutes (λex= 380 nm; λem=460 nm).

Proteins concentrations were normalized to the lowest concentration as determined by the Bradford assay. The lysates were diluted in 1× SDS and heated at 70°C for 10 minutes. The samples are loaded and separated on a 4-12% SDS-Bolt gel (ThermoFisher Scientific) in 1× SDS-PAGE running buffer (G-biosciences, 786-029) at a constant current of 200 V for 25 minutes. The gel was then transferred to a PVDF membrane (Millipore Sigma IPFL00010). Membranes were probed for the expression of ubiquitin (1:200 UbFL-76; Santa Cruz biosciences) and Hsp70 (1:1,000 Hsp70; Enzo Life Sciences). Antibodies against GAPDH (1:5,000 GAPDH; ProteinTech) were used to confirm equivalent loading of proteins.

Flow Cytometry Analysis of MHC-I Peptide Presentation

Upon completion of the reverse time course (step 2.1) cell media was aspirated and washed with chilled 1× PBS. 0.25% Trypsin-EDTA (ThermoFisher Scientific, 25200114) was added to each plate and incubated at 37°C (5% CO2) for four minutes. Trypsin was quenched with cell culture media. Cells were collected and spun down at

1,000 ×g at 4°C for 2 minutes. Media were aspirated and cell pellets were resuspended in growth media. Cells were seeded at 100,000 cells/mL in 96-well, U-bottom plates. A spin down at 500 ×g for 5 minutes was completed. Media was aspirated and chilled 1% FBS in 1× PBS was added for the unlabeled control. Primary antibodies (Y3, 25DI, or Y3+25D1) (Provided by Rock lab, Worcester MA) were added. Cells were incubated for 20 minutes on ice. After 20 minute incubation cells are washed (3 × 5 min spin at 500 ×g) with 1% FBS in 1× PBS. The secondary antibody Anti-IgG1-Alexa 647 (1:500; Thermo Fisher Scientific A-21240) and Anti-IgG2b-PE (1:200; Biolegend 406707) were added and incubated for 20 minutes on ice and protected from light. Analysis by flow cytometry was completed using FACSCalibur (BD Biosciences).Forward and side scatter gates were set and 2000 events were collected per sample, all collection and data analysis done using CellQuest pro (BD Biosciences).

Data Analysis

Protein concentrations measured by the Bradford assay were fit to BSA standards according to a four-parametric curve using SoftMax Pro 7.1 software (Molecular Devices). Peptidase activity was plotted using Graph pad prism version 8. Western blot images were scanned with a Li-COR Odyssey CLx; quantification used the Li-COR Image Studio Lite software package. Data analysis and histogram generation for Flow cytometry was completed CellQuest pro (BD Biosciences).

Chapter III.

Results

The UBL domain of Rad23a Increases Proteasome Activity by Activating Latent Proteasomes

Data from Collins and Goldberg (2020) showed that the Rad23a UBL domain can activate 26S proteasomes. I wanted to determine if the enhanced peptidase activity observed when proteasomes were treated with Rad23a UBL was a result of increased activation of latent proteasomes or due to an increase of the turnover rate (Kcat) of proteasomes. To answer this questions I used an activity probe, MVB-127, which covalently binds to the β5 subunits of the 20S thereby labeling proteasomes with a fluorescent tag. Beyond answering this question, I was also interested in discerning if both the double-capped and single-capped proteasome behaved the same when activated by the UBL domain of Rad23a. To this end, proteasomes labeled with the fluorescent activity probe, MVB127, were analyzed using native PAGE allowing for the visualization of different proteasome sub-populations (i.e. 20S, single-capped, and double-capped proteasomes). All labeling experiments were stopped with the proteasome inhibitor MG-132 at the end of the time course to ensure that proteasomes were only labeled for the designated time. All time points were normalized to the fluorescence signal of T_0 ($T_n - T_0$). To determine the time point at which the proteasomes are saturated with MVB-127, a labeling reaction over 270 minutes was completed (Fig. 1A). Labeling was saturated by 100 minutes for the group treated with the UBL domain of Rad23a and approximately 200 minutes for the untreated control group (Fig. 1B, 1C). This suggests

that Rad23a UBL increases the recruitment of latent proteasomes as the saturation point was reached faster for the treated group than the untreated group with the same end value for both (Fig. 1C; 2B; 2C). Notably, on average, the ratio of double-capped to single-capped proteasomes was 5 fold higher for the group treated with the UBL domain of Rad23a when compared to the untreated group (Fig. 1E). Thus, double-capped proteasomes are more likely to be activated than single-capped proteasomes, probably due to the presence of the second RP which increases the chance of the proteasome binding Rad23a UBL and being activated.

I also discovered that the Rad23a UBL inhibits the activity of the 20S. On average, the untreated 20S had twice the labeled particles than 20S treated with the Rad23a UBL domain (Fig. 1D). The same experiment was repeated once more with similar outcomes (Fig. 2A-2E). Following the two 270 minute time courses, two additional experiments were completed with the labeling reactions stopped at 90 minutes with similar results (Fig. 3-4). Thus, the Rad23a UBL domain increases the labeling kinetics of double-capped and single-capped proteasomes while inhibiting free 20S.

These data suggest that Rad23a UBL activates single-capped and double-capped proteasomes. Specifically, the increase in labeling may plausibly be explained by the following mechanisms: Rad23a UBL activates latent 26S proteasomes by binding Rpn1 of the 19S thereby facilitating substrate entry to the 20S while the Rad23a UBL domain also inhibits 20S (blocks entry of other proteins).

Heat Shock Increases Proteasome Activity in HeLa, HeLa H2-K^b and HeLa H2-K^b NS-OVA Cells

Recently Dr. Donghoon Lee in the Goldberg Lab observed that heat shock (shift from 37°C to 43°C) stimulates 26S proteasome activity and protein degradation. Therefore, this method of activating the proteasome seemed amenable to studying the effects of proteasome stimulation on antigen presentation and it would have the additional benefit of generating discovery data for future experiments. HeLa cells were cultured and incubated at 43°C for varying time periods. Lysates from each time point were analyzed for proteasome activity at 37°C using LLVY-AMC to measure peptidase activity. The results from the peptidase assay were combined from four different experiments. Each incubation point was then normalized to their control (Average T_n - Average T_0) (Fig. 5A). There was an observed 6 fold 8 fold and 20 fold increase of proteasomal activity at two, three and four hours respectively (relative to the one hour incubation at 43°C). These data suggest that heat shock increases proteasomal activity of HeLa cells after a two hour incubation at 43°C.

I tested the effect of increased temperature on MHC-I peptide presentation. To measure MHC-I peptide presentation, I used HeLa H2-K^b and HeLa H2-K^b + NS-OVA cell lines provided by professor Kenneth Rock (Worcester, MA). The HeLa H2-K^b NS-OVA cells internally express ovalbumin. When ovalbumin is degraded by 26S proteasomes it produces SIINFEKL (Serine-Isoleucine-Isoleuicine-Asparagine-Phenylalinine-Glutatmate-Lysine-Leucine) peptides which bind to H2-K^b. The SIINFEKL bound H2-K^b molecules are then expressed on the surface of the cell. The

HeLa H2-K^b cell line only express the H2-K^b surface molecule. I therefore, needed to validate the findings that heat shock stimulated proteasomes in both new cell lines prior to studying presentation of the ovalbumin fragments on the surface (Fig. 5B).

The results from the peptidase assays were combined from two different experiments for the HeLa H2-K^b NS-OVA cells. Each incubation time point was then normalized to their control (Average Tn - Average T0). Like the unmodified HeLa line, lysates from HeLa H2-K^b cells had an increased rate of LLVY hydrolysis at 43°C. HeLa H2-K^b had a 2-fold and 3-fold increase in peptidase activity at three and four hours respectively (relative to the one hour incubation at 43°C) suggesting that proteasomes had been activated by the increased temperature. HeLa H2-K^b NS-OVA yielded mixed results. In one run, there was a small increase in peptidase activity from 2-4 hrs. In a second run, there was no notable change in activity through the first three hours but a strong (2×) increase by the fourth hour. These data suggest that all three cell lines demonstrate an increase in proteasome activity when incubated at 43°C (Fig 5A; 5B). A western blot was performed for each time point using the cell lysates. The gels were probed for the presence of Hsp70, ubiquitin, and GAPDH, which was used as a loading control. The western blot of the HeLa H2-K^b cells treated at 43°C showed induction of Hsp70 which shows that cells expressed the classic heat shock genes and an increased presence of ubiquitinated proteins which implies protein degradation increased as well (Fig. 6A-6D).

The Heat Shock Response Results in Increased MHC-I Peptide Presentation Likely Mediated by the Upregulation of Proteasome Activity

After establishing heat shock as a stimulator of proteasome activity, I wanted to uncover the fate of the peptides that resulted from this upregulation. Given that 26S proteasomes are the primary source of peptides loaded on MHC-I molecules, I hypothesized that an increase in proteasome activity would result in more peptides being formed and shuttled to the MHC-I molecules, ultimately leading to an increase in MHC-I peptide presentation.

Therefore, I analyzed total H2-K^b on the cell surface and H2-K^b presenting SIINFEKL (the ovalbumin derived peptide) by flow cytometry. After incubating the cells at 43°C for three hours, cells were stained with antibodies directed against total surface H2-K^b and H2-K^b presenting SIINFEKL. The total surface presentation of H2-K^b and SIINFEKL-H2-K^b were measured with a flow cytometer (Beckman FACSCalibur). To control for background fluorescence a fluorescence minus one control (FMO) was used to confirm that there was no cross-labeling of the antibodies. FMO allows for the determination of the cut-off point between background and positive population fluorescence (Supplemental Fig. 4). FMO controls were used for all flow cytometry replicates. Because the fluorescent intensity for the total population was logarithmic, the geometric fluorescent intensity (gMFI) was calculated and reported for each replicate.

Surprisingly, when the HeLa H2-K^b cells where incubated for three hours at 43°C the cells had substantially less surface H2-K^b compared to the 37°C control (Fig. 7A). This finding was confirmed by a second replicate where the results showed a similar 60%

decrease in surface H2-K^b (Fig. 7A). However, when HeLa H2-K^b NS-OVA cell were tested, no decrease in surface H2-K^b was observed (Fig. 7B). In fact, in the second set of experiments there was a 20% increase in surface H2-K^b after three hours of heat shock (Fig 7C). Likewise, the transition from 37°C to 43°C for three hours increased the presentation of SIINFEKL peptide bound to surface H2-K^b by nearly 33% (Fig 7C). Together, these data support my hypothesis that heat shock increases the catalytic activity of proteasomes, and is also correlated with increase MHC-I surface presentation.

Chapter IV

Discussion

Here I report different activation kinetics between single-capped and double-capped proteasomes, in response to proteasome activators Rad23a UBL. Importantly, the UBL domain of Rad23a has been shown to activate latent proteasomes, while ATPγS simply promotes activation of previously active particles (Collins and Goldberg, 2020). In an effort to understand the mechanisms by which the UBL domain of Rad23a exerts its effects, I investigated the composition of the newly activated proteasome populations. Specifically, I asked whether the activated proteasomes were singly or doubly capped. Consistent with work completed by Collins and Goldberg which demonstrated that full length Rad23a stimulates peptidase activity of the 26S proteasome through the activation of latent proteasomes, I found that the Rad23a UBL domain preferentially activated double–capped proteasomes.

Next, I wanted to understand the biological consequences of the increase in peptide products brought on by a higher number of activated proteasomes. In particular, I was interested in the relationship between proteasome activation and the immune system. To that end, I probed the effects of heat shock on proteasome activity and quantified subsequent downstream MHC-I presentation.

To test if the UBL domain activates 26S complexes differently if they are single-capped or double-capped, I modified a proteasome labeling assay that uses fluorescently labeled 20S inhibitor, MVB-127 to label single-capped and double-capped 26S. This work required optimizing the concentration of purified proteasomes, MVB-127, and the time needed to maximally label proteasomes with MVB-127. I also verified that reactions

could be frozen at -80°C without compromising the detection of labeled proteasomes (data not shown). With the optimization of this method, I probed the effects of Rad23a UBL on different proteasome populations.

The addition of the UBL domain increased the activation of both single-capped and double-capped proteasomes; however, the double-capped population was activated 30% more than the single-capped population at 90 minutes (Fig. 4F). Thus, the UBL domain of Rad23a may preferentially activate double-capped proteasomes. On average, the ratio of double-capped proteasomes in the groups incubated with the UBL domain of Rad23a were five-fold higher than the untreated groups (Fig. 2 E). Similar observations were also seen in the replicate (Fig. 2E).

Asano and colleagues (2014) found that roughly three-quarters of all proteasomes in neuronal cells are single-capped, compared to around a quarter being double-capped. If increased UBL domain activation was truly stochastic, one would expect more latent single-capped than double-capped proteasomes to be activated due to their greater abundance. Collins and Goldberg (2020) demonstrated that proteolysis is dependent on the association of UBL to Rpn1, work by Martinez-Fonts and colleagues (2020) showed that Rpn13 mediates binding of UBL-UBA proteins and work from Berko and colleagues (2014) showed that Rpn13 is asymmetrically present in double-capped proteasomes. Both, Rpn1 and Rpn13 are ubiquitin receptors for 26S proteasomes. The UBL domain binds to Rpn1, where it mimics the role of ubiquitin, and activates ATP hydrolysis and subsequent degradation if an unlinked unfolded protein is also present, Rpn13 also contributes to binding UBL domains (Collins and Goldberg, 2020; Martinez-Fonts et al., 2020). However, unlike Rpn1, Rpn13 is sub-stoichiometric and is asymmetrically

incorporated to just one end of double-capped proteasomes (Berko et al., 2014; Asano et al., 2015). Perhaps this asymmetry plays a role in the activation of double-capped proteasomes by providing an addition binding site for UBL.

I propose that the observed increase of activation of double-capped proteasomes was mediated by the binding of UBL to Rpn13 and Rpn1, Collins and Goldberg (2020) found that inhibiting the PRU domain of Rpn13 and the UIM domain of Rpn10 result in a loss of UBL binding by about one-third. Although this suggest that Rpn10 and Rpn13 are not essential for the activation of proteasomes by UBL, in the context of my study Rpn10 and Rpn13 are likely implicated in the activation of double-capped proteasomes. Furthermore, Martinez-Fonts (2020) found that proteasomes with Rpn1 and Rpn13 degraded UBL containing peptides 50% more efficiently than Rpn10 proteasomes. The system applied by Martinez-Fonts most closely mimics how the UBL domain interacts with proteasomes in cells compared to using purified UBL in combination with an activity probe (as done in my work). Synthesizing the findings of Collins, Martinez-Fonts and Berko leads me to conclude that Rpn13 and Rpn1 are the subunits most likely responsible for the 30% difference of activation observed between the double-capped and single-capped proteasome (Fig. 4F). While Rpn10 is a UBL binding site, I don't suspect it to be the main binding site for UBL of double-capped proteasomes (Martinez-Fonts and colleagues show that Rpn10 has the lowest affinity for UBL binding), rather I propose that Rpn1 and Rpn13 are the binding site for UBL in double-capped proteasomes. The inherent asymmetry of Rpn13 means that double capped proteasomes have up to three likely binding sites for UBL (Rpn1 on one or both RPs, and Rpn13)

versus the single-capped proteasome that only has one 19S (the UBL domain can bind to Rpn1, and one Rpn13 subunit).

To better elucidate the mechanism by which double-capped proteasomes are activated I suggest that similar experiments be performed using proteasomes with inactivating mutations in Rpn13 and Rpn1. The binding of UBL to Rpn13 can be inhibited by the point mutation at rpn13-pru, likewise a point mutation at rpn1-ARR will inhibit T1 which yeast *Saccharmyces cerevisiae* has been shown to decrease UBL binding (Shi et al., 2016; Collins and Goldberg, 2020).

It is notable that the UBL domain of Rad23a inhibited the labeling of free 20S for all groups (Fig.4F). It seems that the UBL domain blocks the protease activity (blocks the gate) of free 20S subunits while activating latent 26S proteasomes. Western blots confirmed equal loading of 20S for all samples (Supplemental Fig. 1; 2), thus the loss of MVB-127 signal was not due to fewer 20S proteasomes, but rather less active 20S (Supplemental Fig. 3).These data support the activating effects of UBL domains to proteasomes.

These data presented here suggests that heat shock results in increased proteasome activity (Fig. 5). Accordingly, these data suggest the heat-shock mediated increase in proteasome activity could lead to increased MHC-I peptide presentation. Though the mechanism by which this occurs will be an important topic for future research, I propose that the higher rate of protein degradation following heat shock increases the number of peptides available for MHC-I.

To confirm my premise regarding heat shock and proteasome activation, I first performed a time course using HeLa cells incubated at 37°C and 43°C. By three hours, I

identified an 8-fold increase in proteasome activity (Fig. 5A). These observations support the prior observations of the Goldberg lab that increased temperature leads to increases proteasome activation that is even extended after return to 37°C. To test the hypothesis that heat shock also increases MHC-I presentation of antigens, I used the HeLa H2-K^b and HeLa H2-K^b NS-OVA cell lines. After heat shock (3 hours at 43°C) in these cell lines, I tracked surface MHC-I by flow cytometry with antibodies against total surface H-2K^b and SIINFEKL-bound H2-K^b. MHC-I presentation could therefore be quantitatively measured at 37°C and after 3 hours at 43°C. Unexpectedly, HeLa H2-K^b cells had a decrease in H2-K^b on the surface after heat sock (Fig. 8A, 8B). This observation might be explained by the inherent instability of unbound MHC-I molecules. MHC-I molecules are stabilized by the binding of both the peptide, and the peptide loading complex (PLC). PLCs consist of TAP, Crt, ERp57, Tpn, and β2m and are important for binding peptides to MHC-I particles as well as surface presentation (Donaldson and Williams, 2009). Notably, MHC-I molecules that lack a peptide or contain a low affinity peptide are retained in the ER by the PLC. A small fraction of these empty MHC-I molecules does make it to the surface of the cell, but those molecules are unstable even at 37°C and dissociate rapidly (Donaldson and Williams, 2009). It should be expected that unbound MHC-I molecules will dissociate from the cell surface more rapidly at 43°C because of the combined thermal instability and general instability of MHC-I without a bound peptide.

Unlike the HeLa H2-K^b cells, when ovalbumin is expressed (HeLa H2-K^b NS-OVA) total H2-K^b surface presentation increased. Moreover, SIINFEKL bound H2-K^b, surface presentation also increased with heat shock. The first observation was surprising,

because HeLa H2-K^b cells consistently had a decrease of H2-K^b on their surface after heat-shock. Total surface H2-K^b expression would be expected to increase as more peptides are now being generated by the introduction of ovalbumin protein expression. The second finding, provides supporting evidence for the proposed hypothesis. There was approximately a 1.5-fold increase of surface presented SIINFEKL-H2-K^b in the heat treated group relative to the 37°C group (Fig. 7C). Although it may be possible that the cellular stress response induced by the increased temperature caused this increase (i.e. more unfolded proteins, increased ubiquitination). To test if the increased MHC-I surface presentation was in fact a result of increasing proteasome activity I propose testing a different activator of the proteasome and measuring if the same outcome occurs (i.e. PDE5 inhibitors).

In conclusion, this work suggests that the UBL domain preferentially activates double-capped latent proteasomes. Furthermore these data hint that increasing proteasome activity may be a way to increase MHC-I peptide presentation. However, several limitations of this study are worth noting. Native PAGE is notoriously variable and the starting concentrations of each proteasome sub-population was unknown (i.e. I knew the total proteasome concentration, but not fraction of proteasomes that were doubly- or singly-capped). For a future research direction, cryogenic electron microscopy of proteasomes incubated with a UBL domain would result in a higher resolution view of proteasome populations as well as their states (i.e. latent or active). The use of heat shock to activate proteasomes is not sufficient to support this hypothesis. The heat shock response induced by exposure to 43°C is a global response and not specific to the proteasome, as such there are too many other variables to confidently conclude that the

increase of MHC-I presentation was directly caused by proteasome activation. To verify that this was a direct cause of increased proteasome activity, other proteasome activators (i.e PA28) should be used to probe MHC-I peptide presentation. These findings have the potential to stimulate new directions of scholarship as well as contribute to the discovery of novel therapies. A heat treatment could potentially be used to increased MHC-I surface presentation of tumor cells thereby enhancing the patient's antitumor immunity. Further probing into the mechanism by which the heat shock leads to increased MHC-I presentation may also prove promising in the development of novel immunotherapies. The current landscape of drugs that target the proteasome is limited to inhibitors. The development of a proteasome activators could result in advances in treating of various cancers (especially when combined with immunotherapies) or neurodegenerative diseases like Alzheimer's disease and Parkinson's disease.

Appendix I.

Figures

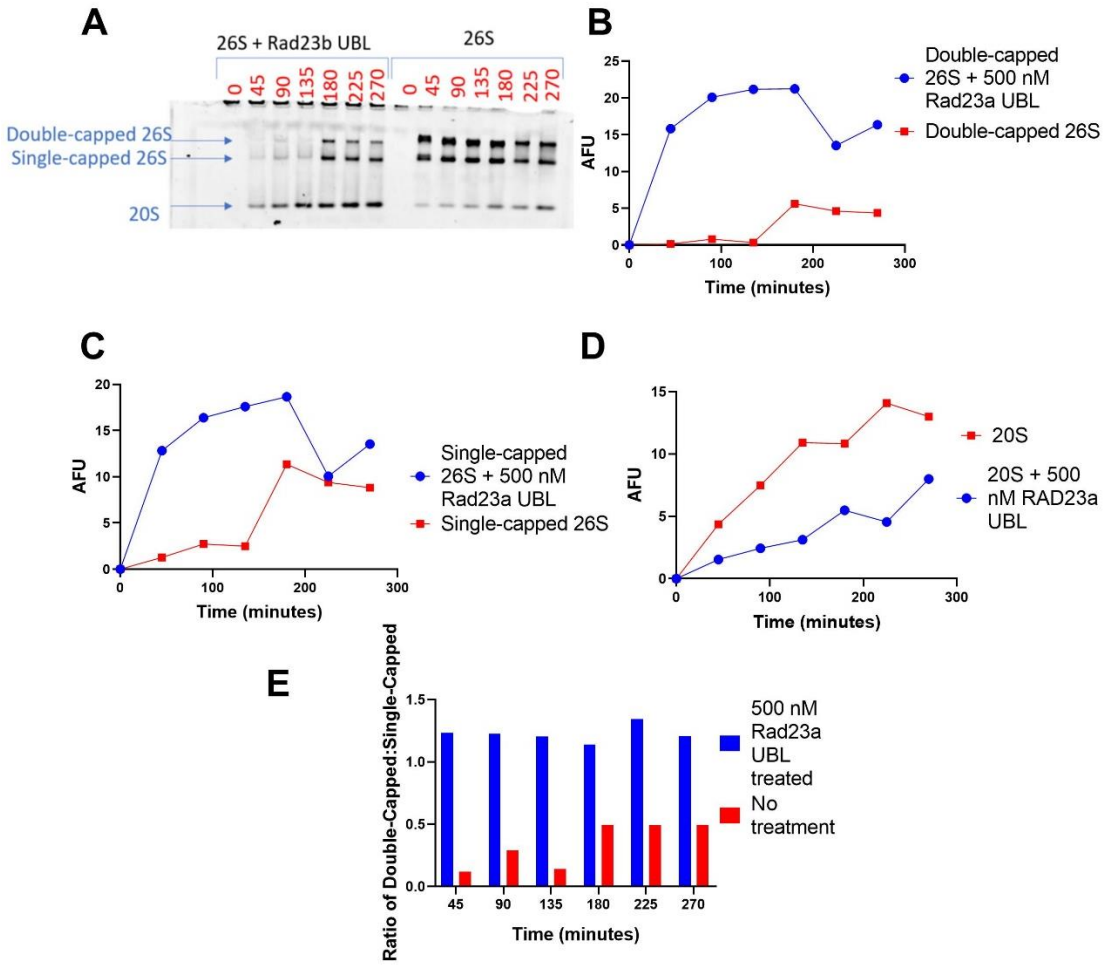

Figure 1. The UBL Domain of Rad23a Activates Latent Proteasomes.

(A) Native PAGE of 12 nM purified 26S MEF-proteasomes incubated with or without 500 nM Rad23a UBL and MVB-127 for indicated time. (B) Quantification of MVB-127 labeling for double-capped proteasomes in panel A. (C) Quantification of MVB-127 labeling for single-capped proteasomes in panel A. (D) Quantification of MVB-127 labeling for 20S proteasomes in panel A. (E) Ratio of single-capped to double-capped proteasomes labeled MVB-127 from quantification in panels B and C.

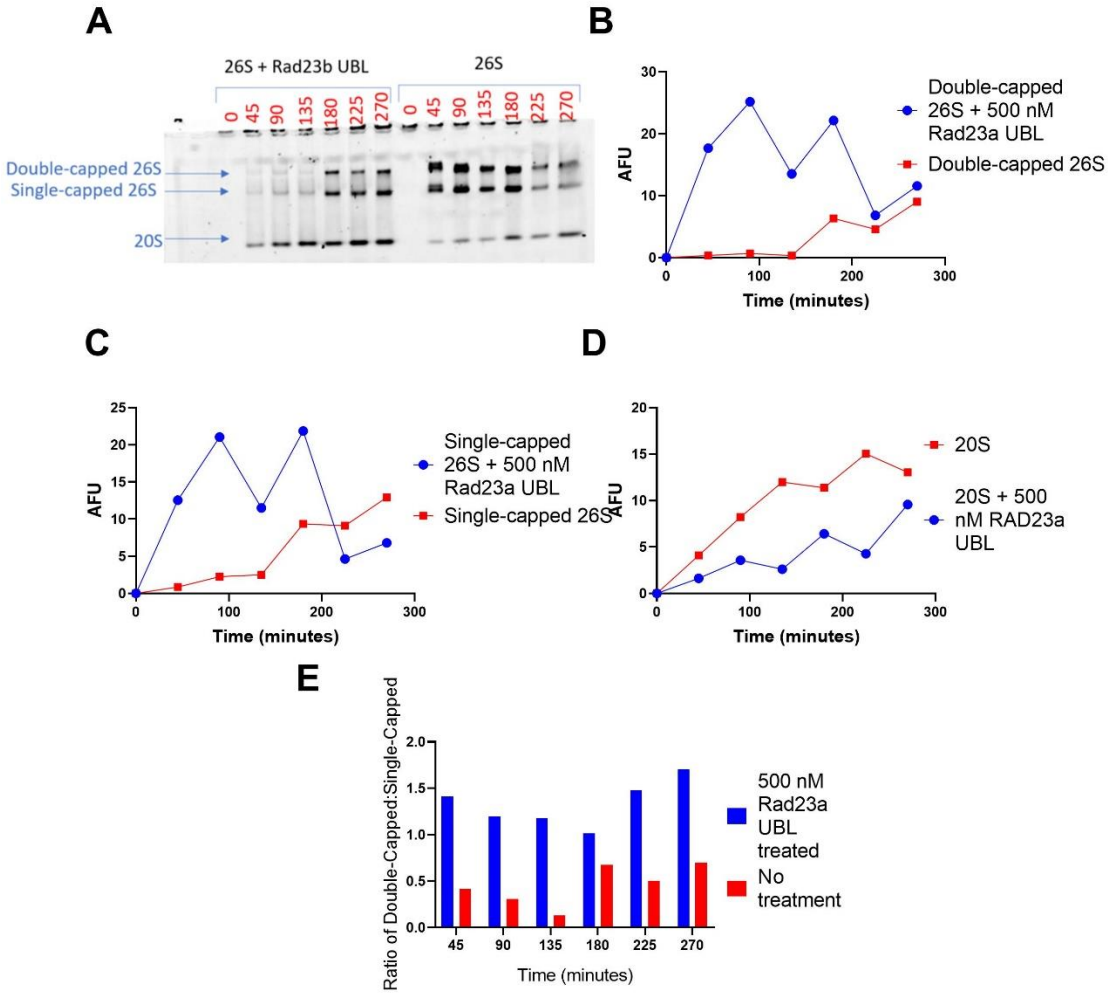

Figure 2. The UBL Domain of Rad23a Activates Latent Proteasomes.

(A) Native PAGE of 12 nM purified 26S MEF-proteasomes incubated with or without 500 nM Rad23a UBL and MVB-127 for indicated time. (B) Quantification of MVB-127 labeling for double-capped proteasomes in panel A. (C) Quantification of MVB-127 labeling for single-capped proteasomes in panel A. (D) Quantification of MVB-127 labeling for 20S proteasomes in panel A. (E) Ratio of single-capped to double-capped proteasomes labeled MVB-127 from quantification in panels B and C.

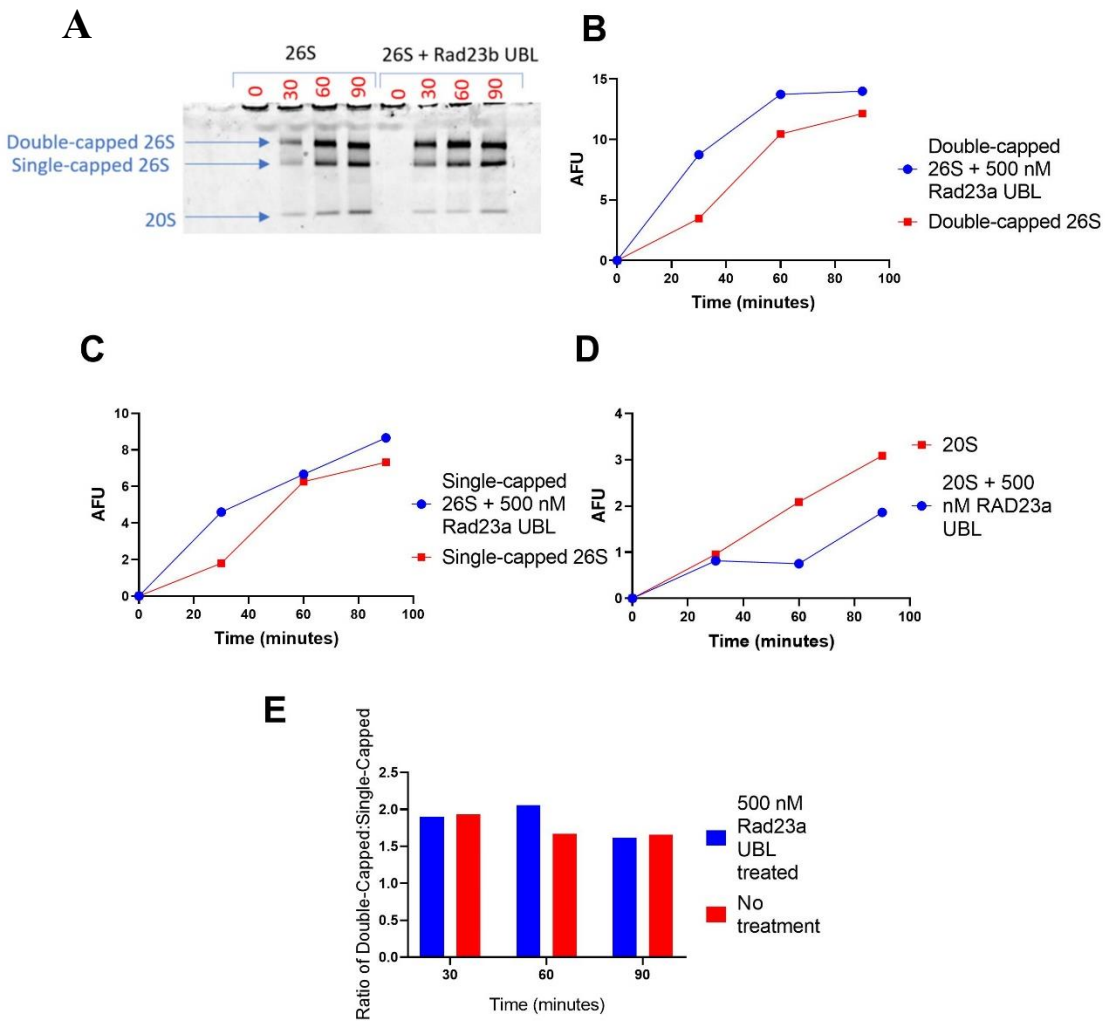

Figure 3. The UBL Domain of Rad23a Activates Latent Proteasomes.

(A) Native PAGE of 12 nM purified 26S MEF-proteasomes incubated with or without 500 nM Rad23a UBL and MVB-127 for indicated time. (B) Quantification of MVB-127 labeling for double-capped proteasomes in panel A. (C) Quantification of MVB-127 labeling for single-capped proteasomes in panel A. (D) Quantification of MVB-127 labeling for 20S proteasomes in panel A. (E) Ratio of single-capped to double-capped proteasomes labeled MVB-127 from quantification in panels B and C.

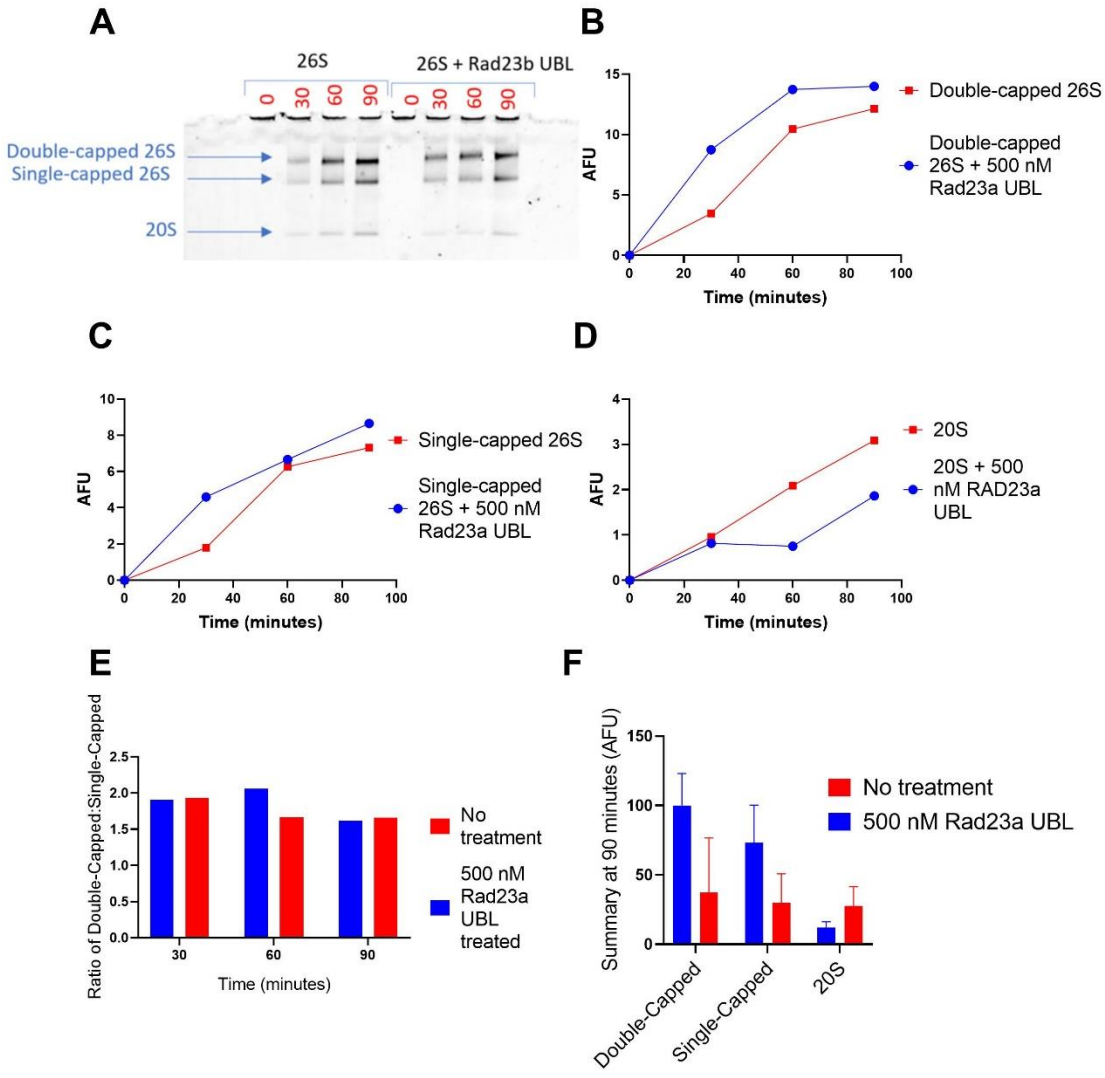

Figure 4. The UBL Domain of Rad23a Activates Latent Proteasomes.

(A) Native PAGE of 12nM purified 26S MEF-proteasomes incubated with or without 500 nM Rad23a UBL and MVB-127 for various time. (B) Fluorescence of double-capped proteasomes labeled with MVB-127 separated by Native PAGE. (C) Fluorescence of single-capped proteasomes labeled with MVB-127 separated by Native PAGE. (D) Fluorescence of 20S proteasomes labeled with MVB-127 separated by native PAGE. (E) Ratio of single-capped to double-capped proteasomes incubated with or without 500 nM Rad23a UBL and MVB-127 followed by a separation on native PAGE. (F) Summary of figures 1-4 at 90 minutes. Data are normalized to the average of the double-capped Rad23a UBL treated group.

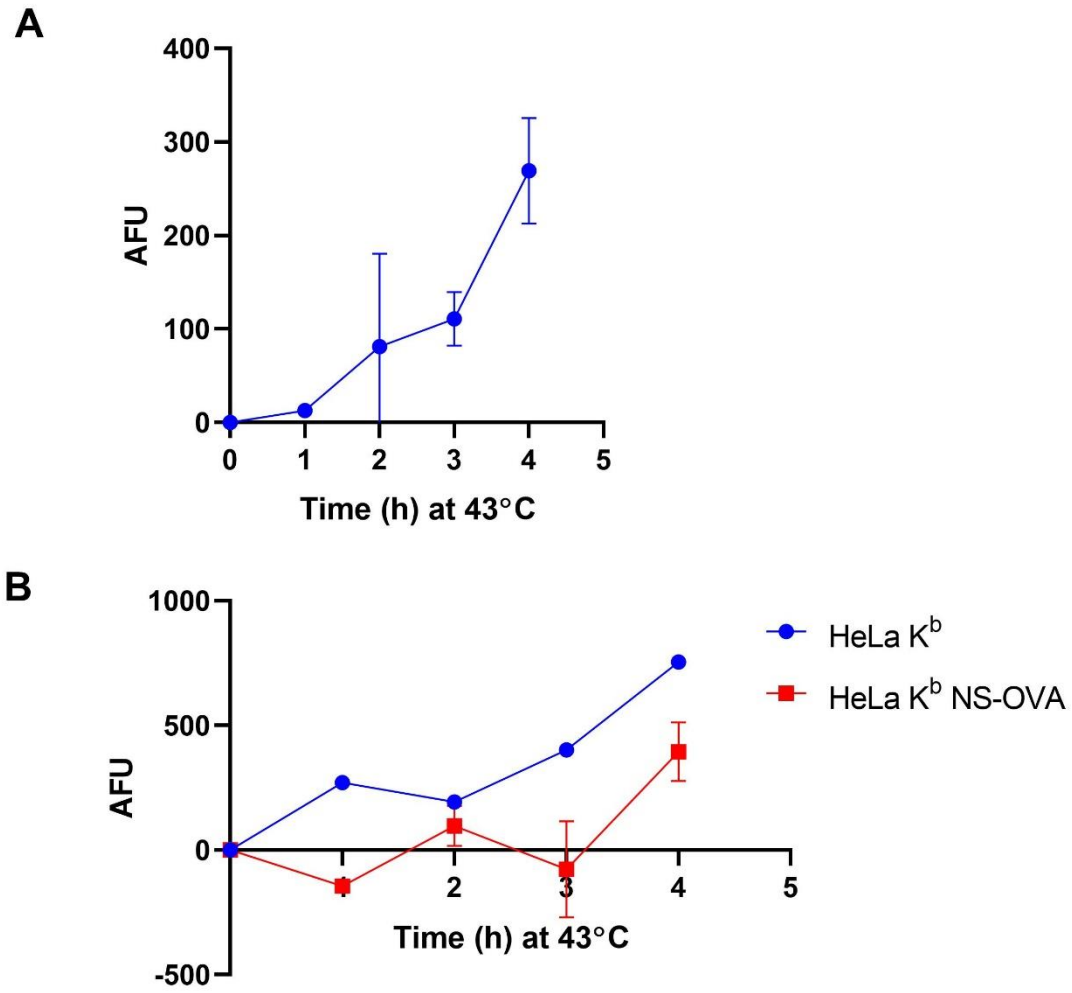

Figure 5. Heat Shock Increases Proteasome Peptidase Activity.

(A) Normalized and combined data from four experiments of the hydrolysis of the small peptide Suc-LLVY-AMC by lysates of HeLa cells incubated at 43°C. (B) Normalized and combined data from four experiments of the hydrolysis of the small peptide Suc-LLVY-AMC by the lysates of HeLa H2-Kb and HeLa H2-Kb NS-OVA cells incubated at 43°C. Error bars represent the SD from n = 4 independent experiments.

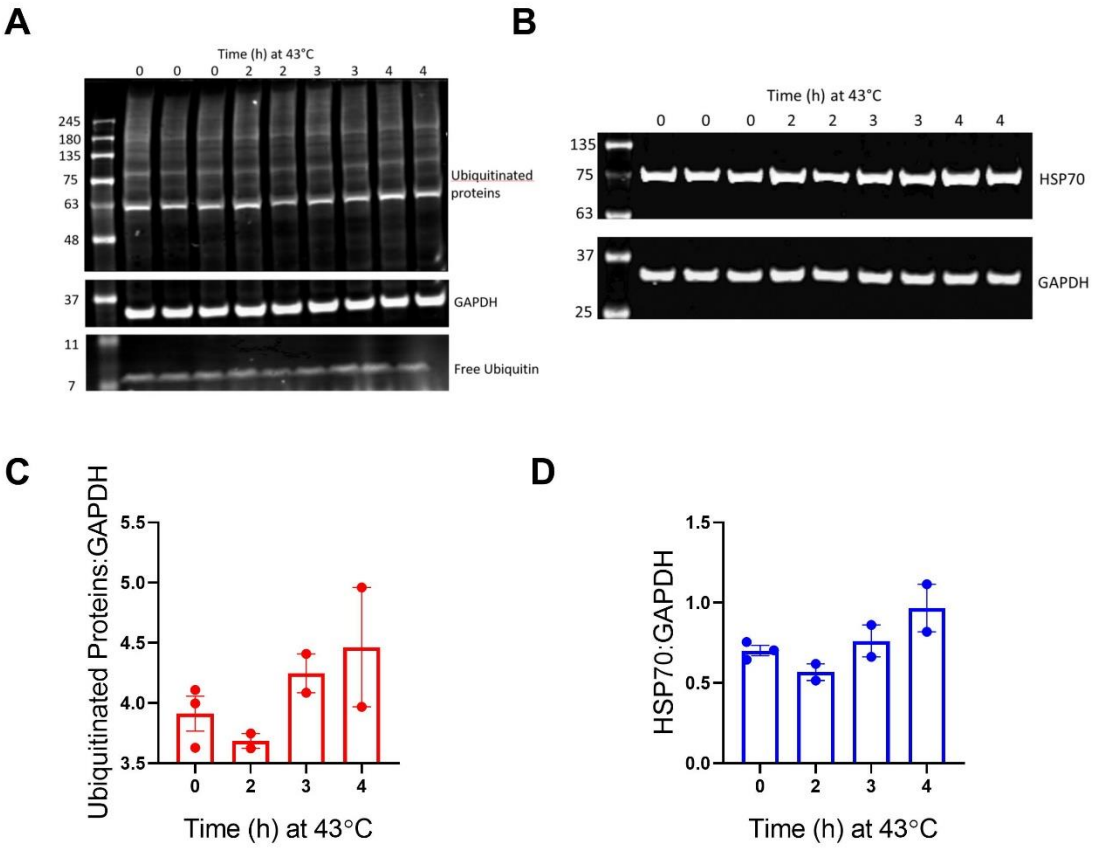

Figure 6. Three hours at 43°C Induces the Heat Shock Response in HeLa H2-K^{b}.

(A) Simultaneous detection of GAPDH and ubiquitinated proteins on a single blot from 43°C incubated HeLa H2-Kb cells. (B) Simultaneous detection of GAPDH and HSP70 proteins on a single blot from 43°C incubated HeLa H2-Kb cells. (C) Relative ratios of ubiquitin to GAPDH for the measurement of protein loading ± SEM (D) Relative ratios of HSP70 to GAPDH for the measurement of protein loading ± SEM.

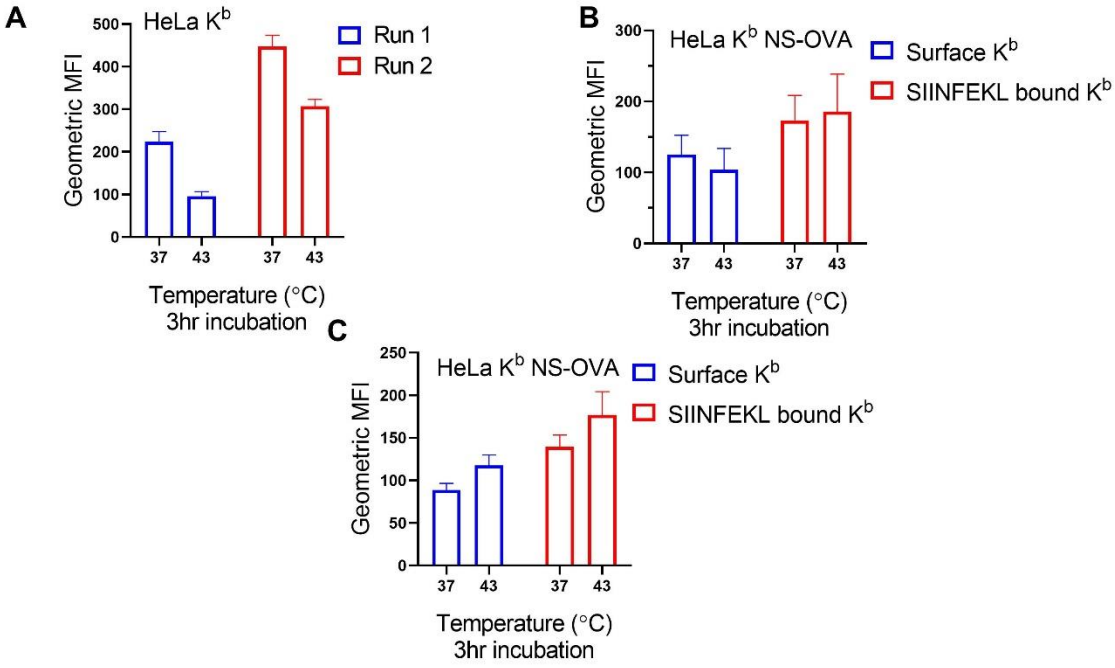

Figure 7. Heat Shock Increases MHC-I Peptide Presentation

(A) Geometric mean fluorescence intensity of run 1 and 2 of surface labeled H2-Kb from the HeLa H2-Kb cell line. (B) Geometric mean fluorescence intensity of run 1 of surface labeled H2-Kb and H2-Kb-SIINFEKL from the HeLa H2-Kb Ns-OVA cell line. (C) Averaged geometric mean fluorescence intensity of surface labeled H2-Kb and H2-Kb-SIINFEKL from the HeLa H2-Kb Ns-OVA cell line from runs 2 - 6 (n = 5) ± SEM.

Appendix II.

Supplemental Figures

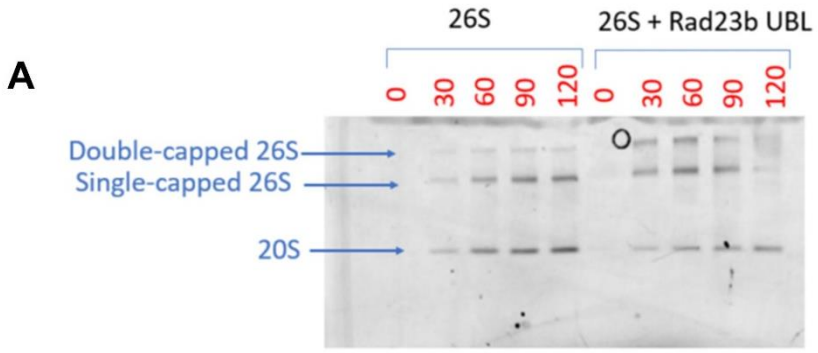

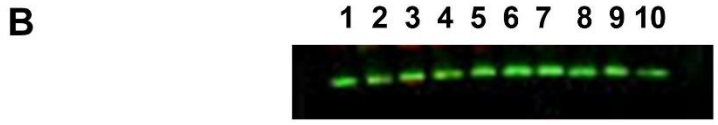

Band	Area
1	30.222
2	28.778
3	27.167
4	29.389
5	30.533
6	29.278
7	31.225
8	27.833
9	29.867
10	28.667

Supplemental Figure 1. 20S is Equally Abundant in Native PAGE Samples.

(A) Native PAGE of 12nM purified 26S MEF-proteasomes incubated with or without 500 nM Rad23a UBL and MVB-127 for various time points. (B) Immunostaining of 20S (PSMB5) particle from native PAGE. Calculated areas are listed by band number, orientation of stain can't be determined. The "circle" in the blot is an artifact of imaging the gel.

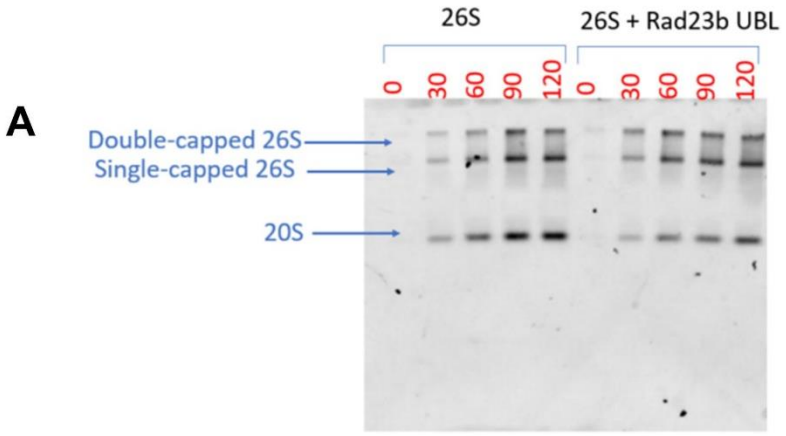

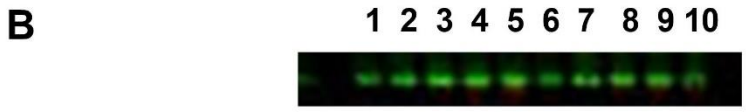

Band	Area
1	8.542
2	7.925
3	8.833
4	7.781
5	8.678
6	9.438
7	8.562
8	9.552
9	7.951
10	8.973

Supplemental Figure 2. 20S is Equally Abundant in Native PAGE Samples.

(A) Native PAGE of 12nM purified 26S MEF-proteasomes incubated with or without 500 nM Rad23a UBL and MVB-127 for various time points. (B) Immunostaining of 20S (PSMB5) particle from native PAGE. Calculated areas are listed by band number, orientation of stain can't be determined.

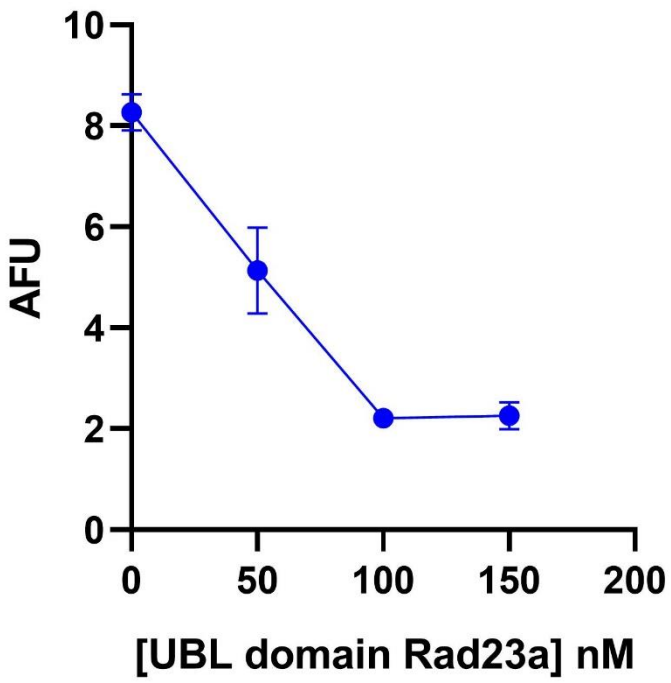

Supplemental Figure 3. The Rad23a UBL Domain Inhibits Free 20S Proteasomes.

Hydrolysis of the small peptide ac-nLPnLD-AMC by 12 nM purified 20S MEF-proteasomes with indicated concentrations of Rad23a UBL reported as mean arbitrary fluorescent units (AFU) ± SD from n = 3 independent experiments.

A

Tube	PE	Alexa-647
Unstained	-	-
PE-FMO	-	+
Alexa-647-FMO	+	-

B

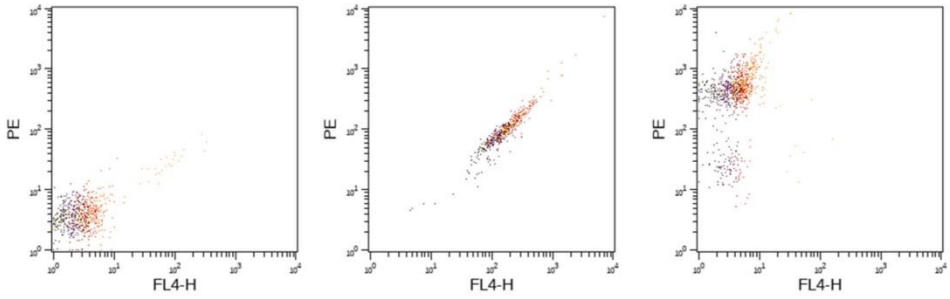

C

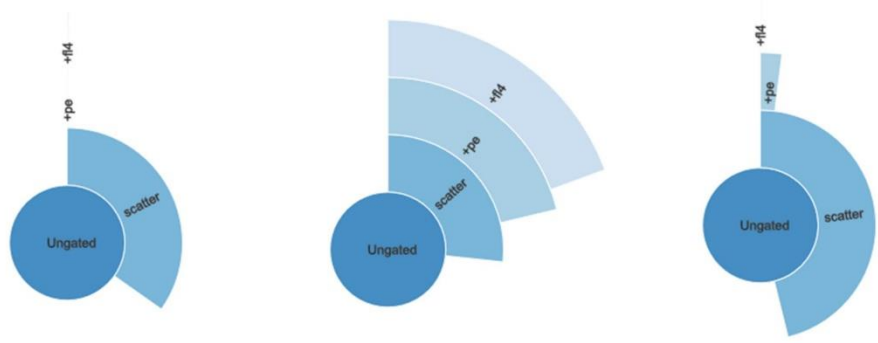

Supplemental Figure 4. FMO Controls Were Used for Both Fluorophores.

(A) Representative table for FMO controls used for Flow cytometry. (B) Representative gated data of FMO controls (B left) unstained cells (B center) double-stained (B right) Alexa-647-FMO. (C) Graphical view of gating (C left) unstained cells (C center) double-stained (C right) Alexa-647-FM

References

Asano, S., Fukuda, Y., Beck, F., Aufderheide, A., Forster, F., Danev, R., & Baumeister, W. (2015). A molecular census of 26S proteasomes in intact neurons. Science,347(6220), 439-442. doi:10.1126/science.1261197

Bennett, J. E., Dolin, R., & Blaser, M. J. (2014). Mandell, Douglas, and Bennetts Principles and Practice of Infectious Diseases. London: Elsevier Health Sciences.

Berko, D., Herkon, O., Braunstein, I., Isakov, E., David, Y., Ziv, T., … Stanhill, A. (2014). Inherent Asymmetry in the 26S Proteasome Is Defined by the Ubiquitin Receptor RPN13. Journal of Biological Chemistry, 289(9), 5609–5618. doi: 10.1074/jbc.m113.509380

Blickwedehl, J., Agarwal, M., Seong, C., Pandita, R. K., Melendy, T., Sung, P., … Bangia, N. (2008). Role for proteasome activator PA200 and postglutamyl proteasome activity in genomic stability. Proceedings of the National Academy of Sciences, 105(42), 16165–16170. doi: 10.1073/pnas.0803145105

Chen, X., Randles, L., Shi, K., Tarasov, S., Aihara, H., & Walters, K. (2016). Structures of Rpn1 T1:Rad23 and hRpn13:hPLIC2 Reveal Distinct Binding Mechanisms between Substrate Receptors and Shuttle Factors of the Proteasome. Structure,24(8), 1257-1270. doi:10.1016/j.str.2016.05.018

Chondrogianni, N., Voutetakis, K., Kapetanou, M., Delitsikou, V., Papaevgeniou, N., Sakellari, M., … Gonos, E. S. (2015). Proteasome activation: An innovative promising approach for delaying aging and retarding age-related diseases. Ageing Research Reviews, 23, 37–55. doi: 10.1016/j.arr.2014.12.003

Collins, G. A., & Goldberg, A. L. (2017). The Logic of the 26S Proteasome. Cell,169(5), 792-806. doi:10.1016/j.cell.2017.04.023

Collins, G. A., & Goldberg, A. L. (2020). Proteins containing ubiquitin-like (Ubl) domains not only bind to 26S proteasomes but also induce their activation. Proceedings of the National Academy of Sciences, 117(9), 4664–4674. doi: 10.1073/pnas.1915534117

Cooper, G. M. (2019). The cell: A molecular approach(8th ed.). New York: Sinauer Associates.

Donaldson, J. G., & Williams, D. B. (2009). Intracellular Assembly and Trafficking of MHC Class I Molecules. Traffic, 10(12), 1745–1752. doi: 10.1111/j.1600-0854.2009.00979.x

Fabre, C., Mimura, N., Bobb, K., Kong, S.-Y., Gorgun, G., Cirstea, D., … Anderson, K. C. (2012). Dual Inhibition of Canonical and Noncanonical NF-κB Pathways Demonstrates Significant Antitumor Activities in Multiple Myeloma. Clinical Cancer Research, 18(17), 4669–4681. doi: 10.1158/1078-0432.ccr-12-0779

Finley, D. (2009). Recognition and Processing of Ubiquitin-Protein Conjugates by the Proteasome. Annual Review of Biochemistry,78(1), 477-513. doi:10.1146/annurev.biochem.78.081507.101607

Fonseca, P. C., & Morris, E. P. (2008). Structure of the Human 26S Proteasome. Journal of Biological Chemistry,283(34), 23305-23314. doi:10.1074/jbc.m802716200

Fort, P., Kajava, A. V., Delsuc, F., & Coux, O. (2015). Evolution of Proteasome Regulators in Eukaryotes. Genome Biology and Evolution,7(5), 1363-1379. doi:10.1093/gbe/evv068

Goldberg, A. L., Cascio, P., Saric, T., & Rock, K. L. (2002). The importance of the proteasome and subsequent proteolytic steps in the generation of antigenic peptides. Molecular Immunology,39(3-4), 147-164. doi:10.1016/s0161-5890(02)00098-6

Hewitt, E. W. (2003). The MHC class I antigen presentation pathway: strategies for viral immune evasion. Immunology, 110(2), 163–169. doi: 10.1046/j.1365-2567.2003.01738.x

Hideshima, T., Bradner, J. E., Wong, J., Chauhan, D., Richardson, P., Schreiber, S. L., & Anderson, K. C. (2005). Small-molecule inhibition of proteasome and aggresome function induces synergistic antitumor activity in multiple myeloma. Proceedings of the National Academy of Sciences, 102(24), 8567–8572. doi: 10.1073/pnas.0503221102

Kim, H. T., & Goldberg, A. L. (2018). UBL domain of Usp14 and other proteins stimulates proteasome activities and protein degradation in cells. Proceedings of the National Academy of Sciences,115(50). doi:10.1073/pnas.1808731115

Kisselev, A. F., Akopian, T. N., Woo, K. M., & Goldberg, A. L. (1999). The Sizes of Peptides Generated from Protein by Mammalian 26 and 20 S Proteasomes. Journal of Biological Chemistry, 274(6), 3363–3371. doi: 10.1074/jbc.274.6.3363

Kisselev, A. F., & Goldberg, A. L. (2001). Proteasome inhibitors: from research tools to drug candidates. Chemistry & Biology, 8(8), 739–758. doi: 10.1016/s1074-5521(01)00056-4

Kisselev, A. F., Callard, A., & Goldberg, A. L. (2006). Importance of the Different Proteolytic Sites of the Proteasome and the Efficacy of Inhibitors Varies with the Protein Substrate. Journal of Biological Chemistry,281(13), 8582-8590. doi:10.1074/jbc.m509043200

Lee, D., Takayama, S., & Goldberg, A. L. (2018). ZFAND5/ZNF216 is an activator of the 26S proteasome that stimulates overall protein degradation. Proceedings of the National Academy of Sciences, 115(41). doi: 10.1073/pnas.1809934115

Li, L., Dong, M., & Wang, X.-G. (2016). The Implication and Significance of Beta 2 Microglobulin. Chinese Medical Journal, 129(4), 448–455. doi: 10.4103/0366-6999.176084

Liepe, J., Marino, F., Sidney, J., Jeko, A., Bunting, D. E., Sette, A., . . . Mishto, M. (2016). A large fraction of HLA class I ligands are proteasome-generated spliced peptides. Science,354(6310), 354-358. doi:10.1126/science.aaf4384

Lowe, J., Stock, D., Jap, B., Zwickl, P., Baumeister, W., & Huber, R. (1995). Crystal structure of the 20S proteasome from the archaeon T. acidophilum at 3.4 A resolution. Science,268(5210), 533-539. doi:10.1126/science.7725097

Martinez-Fonts, K., Davis, C., Tomita, T., Elsasser, S., Nager, A. R., Shi, Y., … Matouschek, A. (2020). The proteasome 19S cap and its ubiquitin receptors provide a versatile recognition platform for substrates. Nature Communications, 11(1). doi: 10.1038/s41467-019-13906-8

Morozov, A. V., & Karpov, V. L. (2018). Biological consequences of structural and functional proteasome diversity. Heliyon,4(10). doi:10.1016/j.heliyon.2018.e00894

Parag, H., Raboy, B., & Kulka, R. (1987). Effect of heat shock on protein degradation in mammalian cells: involvement of the ubiquitin system. The EMBO Journal, 6(1), 55–61. doi: 10.1002/j.1460-2075.1987.tb04718.x

Peth, A., Besche, H. C., & Goldberg, A. L. (2009). Ubiquitinated Proteins Activate the Proteasome by Binding to Usp14/Ubp6, which Causes 20S Gate Opening. Molecular Cell, 36(5), 794–804. doi: 10.1016/j.molcel.2009.11.015

Peth, A., Kukushkin, N., Bossé, M., & Goldberg, A. L. (2013). Ubiquitinated Proteins Activate the Proteasomal ATPases by Binding to Usp14 or Uch37 Homologs. Journal of Biological Chemistry, 288(11), 7781–7790. doi: 10.1074/jbc.m112.441907

Rabl, J., Smith, D. M., Yu, Y., Chang, S.-C., Goldberg, A. L., & Cheng, Y. (2008). Mechanism of Gate Opening in the 20S Proteasome by the Proteasomal ATPases. Molecular Cell, 30(3), 360–368. doi: 10.1016/j.molcel.2008.03.004

Rock, K. L., Gramm, C., Rothstein, L., Clark, K., Stein, R., Dick, L., … Goldberg, A. L. (1994). Inhibitors of the proteasome block the degradation of most cell proteins and the generation of peptides presented on MHC class I molecules. Cell, 78(5), 761–771. doi: 10.1016/s0092-8674(94)90462-6

Rock, K. L., Reits, E., & Neefjes, J. (2016). Present Yourself! By MHC Class I and MHC Class II Molecules. Trends in Immunology, 37(11), 724–737. doi: 10.1016/j.it.2016.08.010

Schmidt, M., & Finley, D. (2014). Regulation of proteasome activity in health and disease. Biochimica Et Biophysica Acta (BBA) - Molecular Cell Research,1843(1), 13-25. doi:10.1016/j.bbamcr.2013.08.012

Schrader, E. K., Harstad, K. G., & Matouschek, A. (2009). Targeting proteins for degradation. Nature Chemical Biology,5(11), 815-822. doi:10.1038/nchembio.250

Schreiner, P., Chen, X., Husnjak, K., Randles, L., Zhang, N., Elsasser, S., . . . Groll, M. (2008). Ubiquitin docking at the proteasome through a novel pleckstrin-homology domain interaction. Nature,453(7194), 548-552. doi:10.1038/nature06924

Scruggs, S. B., Zong, N. C., Wang, D., Stefani, E., & Ping, P. (2012). Post-translational modification of cardiac proteasomes: Functional delineation enabled by proteomics. American Journal of Physiology-Heart and Circulatory Physiology,303(1). doi:10.1152/ajpheart.00189.2012

Shi, Y., Chen, X., Elsasser, S., Stocks, B. B., Tian, G., Lee, B.-H., … Walters, K. J. (2016). Rpn1 provides adjacent receptor sites for substrate binding and deubiquitination by the proteasome. Science, 351(6275). doi: 10.1126/science.aad9421

Shibatani, T., Carlson, E. J., Larabee, F., Mccormack, A. L., Früh, K., & Skach, W. R. (2006). Global Organization and Function of Mammalian Cytosolic Proteasome Pools: Implications for PA28 and 19S Regulatory Complexes. Molecular Biology of the Cell, 17(12), 4962–4971. doi: 10.1091/mbc.e06-04-0311

Sledz, P., Unverdorben, P., Beck, F., Pfeifer, G., Schweitzer, A., Forster, F., & Baumeister, W. (2013). Structure of the 26S proteasome with ATP- S bound provides insights into the mechanism of nucleotide-dependent substrate translocation. Proceedings of the National Academy of Sciences, 110(18), 7264–7269. doi: 10.1073/pnas.1305782110

Stadtmueller, B. M., & Hill, C. P. (2011). Proteasome Activators. Molecular Cell, 41(1), 8–19. doi: 10.1016/j.molcel.2010.12.020

Tanaka, K. (2009). The proteasome: Overview of structure and functions. Proceedings of the Japan Academy, Series B,85(1), 12-36. doi:10.2183/pjab.85.12

Weissman, A. M. (2001). Themes and variations on ubiquitylation. Nature Reviews Molecular Cell Biology,2(3), 169-178. doi:10.1038/35056563